Similarity spectra analysis of high-performance jet aircraft noise

Tracianne B. Neilsen,[a] Kent L. Gee, and Alan T. Wall

Department of Physics and Astronomy, N283 ESC, Brigham Young University, Provo, Utah 84602

Michael M. James

Blue Ridge Research and Consulting, 15 West Walnut Street, Suite C, Asheville, North Carolina 28801

Noise measured in the vicinity of an F-22A Raptor has been compared to similarity spectra found previously to represent mixing noise from large-scale and fine-scale turbulent structures in laboratory-scale jet plumes. Comparisons have been made for three engine conditions using ground-based sideline microphones, which covered a large angular aperture. Even though the nozzle geometry is complex and the jet is nonideally expanded, the similarity spectra do agree with large portions of the measured spectra. Toward the sideline, the fine-scale similarity spectrum is used, while the large-scale similarity spectrum provides a good fit to the area of maximum radiation. Combinations of the two similarity spectra are shown to match the data in between those regions. Surprisingly, a combination of the two is also shown to match the data at the farthest aft angle. However, at high frequencies the degree of congruity between the similarity and the measured spectra changes with engine condition and angle. At the higher engine conditions, there is a systematically shallower measured high-frequency slope, with the largest discrepancy occurring in the regions of maximum radiation. © 2013 Acoustical Society of America. [http://dx.doi.org/10.1121/1.4792360]

I. INTRODUCTION

A principal contributor to the radiated noise from supersonic jets is turbulent mixing noise, which occurs as a result of fine and large-scale turbulent structures.[1,2] Extensive examination of a large database of supersonic laboratory-scale jet data led to the empirical formulation of a similarity spectrum for each type of noise.[3] While these similarity spectra have been shown to match the spectra of laboratory-scale jets at a variety of operating conditions,[4,5] less is known about their applicability to the noise radiated by high-power engines installed in military aircraft. This paper contains a comparison of the similarity spectra and noise from a Pratt-Whitney F119-PW100 turbofan engine installed in a Lockheed Martin/Boeing F-22A Raptor (abbreviated as F-22 hereafter). The comparison is carried out for multiple engine powers and a variety of angles and distances in the vicinity of the aircraft.

An experimental study of supersonic jet noise reported by Schlinker[6] and Laufer *et al.*[7] in the mid 1970s indicated that the sound radiated to the sideline of a jet and in the highest amplitude region are distinctly different.[6] In Ref. 8, the two sources proposed by Schlinker were shown to correspond to the fine and large-scale turbulent structures described by Tam *et al.*[3] In addition to observing the two types of turbulent mixing noise, Tam *et al.*[3] examined the NASA Langley Research Center's Jet Noise Laboratory database and investigated the self similarity of the noise spectra from jets operated at different conditions. Far-field data from a range of cold and heated supersonic laboratory-scale jets were used to develop two similarity spectra that match the primary features of the noise from the fine-scale structures (FSSs) and

the large-scale structures (LSSs). The LSS spectrum, which has a relatively narrow peak and power-law decay on both sides, was reported to fit the data for aft angles. On the other hand, the FSS similarity spectrum, with its broader peak and a more gradual roll-off at both high and low frequencies, matched the radiated spectra to the sideline direction. Tam *et al.*[3] proposed that jet noise at any radiation angle can be represented as a sum of LSS and FSS similarity spectra. Two recent review articles by Tam *et al.*[4] and Viswanathan[5] discuss how the similarity spectra have been compared to a wide variety of laboratory-scale jets.

There are far fewer comparisons between full-scale jet engines and similarity spectra, which motivates the present study. Most notable is the investigation by Schlinker *et al.*,[9] who compared the LSS spectral shape with the measured spectra at aft angles for a high- performance jet engine with a round nozzle at its full-thrust set point. They observed that, although the LSS spectrum matched the lower portion of the measured spectra reasonably well, the measured high-frequency spectral slopes were significantly shallower (∼20 dB/decade) than the LSS spectrum's roll-off (∼28 dB/decade). The authors also pointed out that a similar slope exists for unheated Mach-2.47 (Ref. 6) and heat-simulated Mach 1.5 (Ref. 10) laboratory-scale data. A similar high-frequency slope has been observed in the noise measured 23 m from a static F-22 at afterburner.[11]

The purpose of this paper is to examine how well the similarity spectra, developed using far-field data, describe the near-field properties of the noise from an installed, high-power jet engine. This investigation hopes to shed light on whether the far-field discrepancy between the similarity spectra and high-power jet engines in the region of maximum radiation, observed previously, persists in the near field. Specifically, the similarity spectra corresponding to the LSS and

[a]Author to whom correspondence should be addressed. Electronic mail: tbn@byu.edu

FSS mixing noise are compared to noise recorded from an installed, F119-PW100 engine at intermediate (80%), military (100%), and afterburner conditions. In Sec. II, the two similarity spectra for jet noise are described, followed by a review of cases where the similarity spectra have been shown to match laboratory-scale data. Section III contains a brief description of an F-22 noise measurement. Section IV begins with an examination of the (polar) angular dependence of the radiated sound field as observed 11.6 m to the sideline of the jet exhaust for four engine conditions. Comparison between measured data at ground-based microphones and the similarity spectra are presented. The relative contributions of the two similarity spectra as functions of engine condition and angle, as well as systematic discrepancies, are explored.

II. BACKGROUND

A. Similarity spectra model

The noise radiated from the fine and large-scale turbulent structures is believed to have different properties. The FSS, distributed throughout the plume, are relatively compact sources and radiate omnidirectionally. The LSS have larger spatial coherence properties and thus produce directional sound radiation. Consequently, in the direction of maximum radiation, noise from the large-scale structures dominates the sound field. The noise radiated from the fine-scale structures is, therefore, most likely to be detected to the sideline of the jet. The relative contribution of these two noise sources depends on Mach number, jet temperature, and radiation angle.[4,12]

According to Tam's two-source model, there is a similarity spectrum that represents each type of turbulent mixing noise in jets: F for the LSS and G for the FSS. The similarity spectra are functions of the frequency ratio $f_r = f/f_p$, where f_p is the spectral peak (or characteristic) frequency. The F and
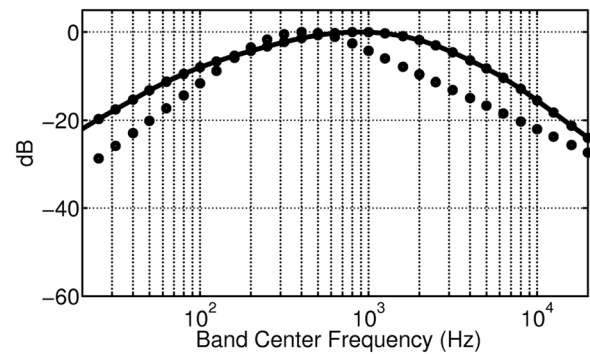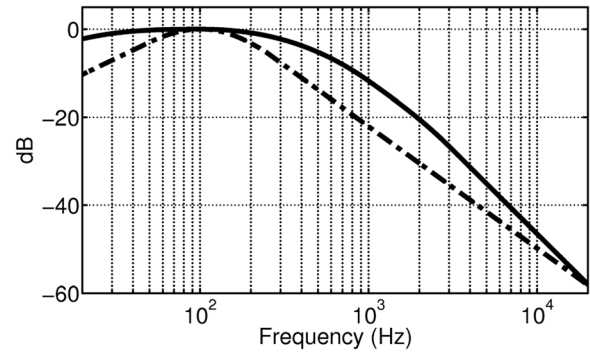

FIG. 1. Similarity spectra for (a) narrowband and (b) one-third octave band corresponding to the fine-scale turbulent structure, G (solid line) and the large-scale turbulent structures, F.

G similarity spectra, for the same peak frequency, are illustrated in Fig. 1(a). The correct equations for computing the similarity spectra are found in Ref. 13. On a decibel scale, the overall shape of the F similarity spectrum is defined with straight lines on the low- and high-frequency ends and cubic equations in two mid-frequency ranges as

$$10\log(F) = \begin{cases} 2.54 + 18.40\log(f_r), & f_r < 0.5, \\ -38.9(\log(f_r))^2 - 16.9(\log(f_r))^3, & 1.0 > f_r \geq 0.5, \\ 1.07\log(f_r) - 45.30(\log(f_r))^2 + 21.41(\log(f_r))^3, & 2.5 > f_r \geq 1.0, \\ 5.64 - 27.75\log(f_r), & f_r \geq 2.5. \end{cases} \tag{1}$$

The G similarity spectrum has a more rounded shape, which requires functional fits for six frequency ranges, expressed as

$$10\log(G) = \begin{cases} 9.90 + 14.91\log(f_r), & f_r < 0.05, \\ -3.5 + 11.87\log\left(\frac{20}{3}f_r\right) + 2.12\left(\log\left(\frac{20}{3}f_r\right)\right)^2 + 7.52\left(\log\left(\frac{20}{3}f_r\right)\right)^3, & 0.15 > f_r \geq 0.05, \\ -1.06(\log(f_r))^2 + 4.98(\log(f_r))^3, & 1.0 > f_r \geq 0.15, \\ -8.15(\log(f_r))^2 - 3.65(\log(f_r))^3, & 10 > f_r \geq 1.0, \\ -11.80 - 27.25\log\left(\frac{1}{10}f_r\right) - 0.81\left(\log\left(\frac{1}{10}f_r\right)\right)^2 - 14.85\left(\log\left(\frac{1}{10}f_r\right)\right)^3, & 30 > f_r \geq 10, \\ 29.78 - 38.17\log(f_r), & f_r \geq 30. \end{cases} \tag{2}$$

The similarity spectra in Eqs. (1) and (2) are normalized such that the (decibel) levels are equal to zero when $f_r = 1$.

When comparing the similarity spectra to the F-22 data, the narrowband values are calculated and then converted to one-third octave (OTO) band spectra, similar to the procedure used by Viswanathan.[12] Figure 1(b) shows how the shapes of the similarity spectra [shown in Fig. 1(a)] change when converted to OTO bands and renormalized to equal zero at $f_r = 1$. The location of the peak in the OTO band G spectrum shifts nearly a decade because of the relative number of frequencies in each band and the broad nature of the narrowband FSS spectral shape. In addition, because of the OTO band processing, the high-frequency slope, which is -27.8 dB/decade for the narrowband LSS spectrum in Fig. 1(a), is -17.8 dB/decade for the OTO band LSS spectrum in Fig. 1(b). This slope is relevant to investigating the roll-off of the high-frequency portions of the engine spectra. For the analyses in this paper, the OTO band similarity spectra are shifted to match the peak frequency and level of the F-22 spectra for different engine conditions measured at a variety of locations.

Often only one of the similarity spectra is required to model the spectral shape of the measured noise: F in the direction of maximum radiation and G to the sideline. In such cases, the appropriate normalized similarity spectrum is simply raised to match the peak level of the measured spectrum. In a few cases[3,4,14–16] a combination of the F and G similarity spectra has been shown to fit the data at angles between sideline and the principal radiation region. In such cases, the noise spectrum at an angle θ is given as

$$S(f, \theta) = [A(\theta)F(f_{r,F}) + B(\theta)G(f_{r,G})]\left(\frac{D_j}{r}\right)^2. \tag{3}$$

This is a useful expression when the nozzle diameter, D_j, and distance from the jet noise sources, r, are well known, and the measurements are taken in the far field where spherical spreading can be assumed. Then, $A(\theta)$ and $B(\theta)$, which represent amplitude-scaled directivity functions, are the effective LSS and FSS noise source strengths.[3] A recently developed jet noise source model was built explicitly upon the idea of summing distributions of incoherent simple sources and coherent, directionally radiating sources, thus mimicking essential FSS and LSS properties.[17]

Because the current work investigates the applicability of the F and G spectra in the vicinity of an extended engine exhaust, it cannot be assumed that the noise is spherically spreading along propagation radials. Thus, the angular and radial dependence cannot be separated explicitly, as in Eq. (3). Subsequently, the source strengths A and B are replaced by $a(\mathbf{r})$ and $b(\mathbf{r})$, which represent the contributions of the LSS and FSS noise at some arbitrary position, $\mathbf{r}$. The noise spectrum at a distance r and angle θ from the jet, $S(f, \mathbf{r})$, can be thus expressed in terms of the similarity functions and coefficients that quantify the strength of each type of mixing noise at that location. The summation of the two contributors may be written as

$$S(f, \mathbf{r}) = a(\mathbf{r})F(f_{r,F}) + b(\mathbf{r})G(f_{r,G}). \tag{4}$$

In practice, f_r can be different for the F and G similarity spectra, hence the need for the additional subscripts F and G in Eqs. (3) and (4). For simplicity, the contribution to the noise spectrum from the large-scale structures at the location $\mathbf{r}$ is defined as $LSS(f, \mathbf{r}) = a(\mathbf{r})F(f_{r,F})$ and from the fine-scale structures is $FSS(f, \mathbf{r}) = b(\mathbf{r})G(f_{r,G})$. While the contribution from a single component can be expressed on a decibel scale, the total predicted spectral levels are given by $10\log S(f, \mathbf{r}) = 10\log(LSS(f, \mathbf{r}) + FSS(f, \mathbf{r}))$.

B. Applications

Data from many laboratory-scale jet experiments agree relatively well with the similarity spectra. In the original study, Tam, Golebowski, and Seiner[3] explored supersonic jets (Mach 1.37 to 2.24) with circular nozzles that were operated at ideally and imperfectly expanded conditions. Data from both cold and heated jets ($T_{ratio} = 1.0$–4.9, where T_{ratio} is the ratio of the jet temperature to the ambient air temperature) were scaled to 100 D_j, where D_j is the nozzle diameter.

More recent reports on cold and heated, subsonic and supersonic laboratory jet data have also shown a mostly favorable comparison with the similarity spectra. Tam et al.[8] examined Schlinker's dissertation data[6] on unheated jets operated at Mach 1.47, 1.97, and 2.47. To the sideline, the data were well represented by the FSS spectrum (see Fig. 3 in Ref. 8). In the maximum noise direction, there was good agreement with the LSS spectrum, except at the highest frequencies for Mach 2.47, which has closer to a 20 dB/decade roll off (see Fig. 2 in Ref. 8). In addition, Tam et al. in Ref. 4 have summarized the excellent agreement between laboratory-scale data for Mach 0.7, 1.5, and 1.96 jets with $T_{ratio} = 1.8$ and the similarity spectra. Specifically, the FSS spectrum agrees with the data at 80°, 90°, 100°, while the LSS spectrum matches at 130° and 140°. In addition, many studies on subsonic and supersonic jets conducted by Viswanathan have shown, in general, support for the similarity spectra.[5,12,14]

While the FSS spectrum matches sideline data, and the LSS spectrum matches farther aft, there is a transition region where a combination of the LSS and FSS spectra is required to replicate the data, indicating that both types of mixing noise are contributing significantly to the sound field. For example, Tam et al.[4] show that a combination of FSS and LSS provide a good representation of the data at 110° and 120° (see Fig. 3 of Ref. 4). Figure 6 of Ref. 4 shows the relative contributions of the FSS and LSS spectra that yield the best match with the data as a function of angle (50°–160°) for Mach 0.3, 0.6, 0.9, 1.5, and 2.0 data with $T_{ratio} = 1.0$ and 2.2. While no measure is given to quantify the match between the resulting similarity spectra, it is worthwhile noting that the angles at which combinations of FSS and LSS spectra are needed changes with Mach number.[5,12] Specifically, the angle at which a combination of LSS and FSS is first needed lessens as Mach number increases, which corresponds with the direction of maximum radiation moving farther forward. In addition, the transition region between FSS and LSS narrows with increasing Mach number.

The effect of the nozzle geometry on the radiated noise has also been investigated. Tam's work was continued in Ref. [18] with studies of supersonic jets from elliptical nozzles, with an aspect ratio of 3, and rectangular nozzles, with an aspect ratio of 7.6. For a Mach 2.0 jet with a $T_{ratio} = 1.8$, the LSS spectrum had good agreement at $150°$ and the FSS at $90°$ along both the major and minor axes. Similarly, Tam and Zaman[13] found that the similarity spectra matched data measured for cold, subsonic jets with elliptical, rectangular, and tabbed circular nozzles (at $r = 100\,D_j$). In addition, Dahl and Papamoschou[16] found excellent agreement for heated, supersonic coaxial (dual-stream) jet noise for both FSS at sideline and LSS farther aft at $80\,D_j$ by doing a least-squares fit of the similarity spectra to the measurement. Robust agreement between the FSS and sideline noise from coaxial jets operating at a variety of conditions was reported in Ref. [12]. The conditions of the coaxial jet had a greater effect on the spectral shape in the principal radiation direction, so only the LSS often appeared to disagree with measured spectra.

Although relatively good agreement was found in the aforementioned cases, two extra issues need to be considered. First, the effects of atmospheric absorption were not addressed explicitly in the development of the similarity spectra. Evidence of atmospheric absorption in a measured far-field spectrum would appear as an exponential roll-off at high frequencies, where the relative definition of "high" is determined by propagation range. In particular, the effect of atmospheric absorption on the high-frequency portion of the spectrum from subsonic and supersonic jets was investigated by Viswanathan in Ref. [12]. It was found that by converting the data to standard day conditions ($25\,°C$ with a relative humidity of 70%) and including corrections for spherical spreading and atmospheric absorption to $100\,D_j$, a better match was achieved between the high-frequency portion of the FSS spectrum and the sideline data.[12]

The second discrepancy, discussed by Schlinker *et al.*,[9] is the shallower high-frequency slope, often seen in comparisons between the LSS spectrum and the supersonic jet data in the region of maximum radiation. This was actually originally noted by Tam *et al.*[3] when they first formulated the similarity spectra. In reference to the heated, Mach 2.0 jet spectrum at $160°$ (cf. Fig. 3 in Ref. [3]) the authors stated, "At very high frequencies, the agreement is less good in some cases. At this time, it is not clear what is the cause of this discrepancy."[3] However, this observation has been neglected in subsequent studies. In our examination of some publications, it appears that the similarity spectra have been shifted in a visual or a least-squares sense such that the agreement in the high-frequency portion of the spectrum was improved at the expense of a worse fit in the peak-frequency region.[3,15–17] This approach is not taken herein because of the quality of the match in the peak-frequency region that can be obtained by allowing some mismatch in the high-frequency slope.

III. EXPERIMENT

An extensive experiment was conducted to measure the noise produced by an F119-PW100 engine installed on a static F-22A Raptor. The engine nozzle exit is nominally
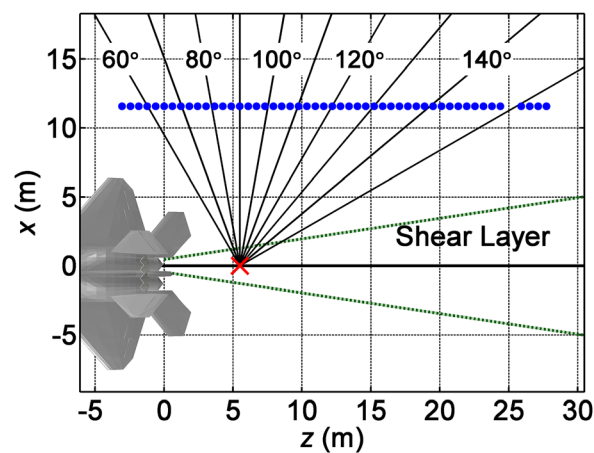

FIG. 2. (Color online) Schematic of the measurement locations relative to the aircraft. The elements of the linear ground-based microphone array at $11.7\,m$ from the jet centerline are marked by dots. The distances r and angles θ used in this paper are measured relative to the "$\times$" located $5.5\,m$ downstream of the nozzle exit, which estimates the maximum aeroacoustic source region, z_0. (The $+y$-axis is out of the page.)

rectangular, but the shape is influenced by the thrust vectoring paddles. The engine closest to the measurement microphones was cycled through four power conditions: idle, intermediate (80%), military (100%), and full afterburner, while the other engine was held at idle. Additional details regarding of the aerodynamics of the jet flow are not available. Although only a brief review of measurement procedures is given here, comprehensive descriptions may be found in Refs. [19] and [20]. The abundant data provide insights into the nature of the sound field in the vicinity of the aircraft. Figure [2] is a schematic of the portion of the experiment pertinent to this paper.

The source-receiver distances and angles in this paper are calculated relative to the engine inlet and an origin located $5.5\,m$ (roughly 8–10 nozzle diameters) downstream from the jet nozzle exit, which is referred to as z_0 and denoted with a "$\times$" in Fig. [2]. The scaled distance to this origin is about the same as in Refs. [11] and [21] and is chosen to approximate the location of the dominant aeroacoustic source region, in general accordance with various source characterization analyses including beamforming,[9] collapse of data along propagation radials,[11] near shear-layer power distribution,[22] wave packets,[15] and near-field acoustical holography.[23] Table [I] gives a comparison of the angles based on placing the origin at the dominant source region θ and the angles determined using an origin underneath the nozzle exit in Fig. [2], θ_e. Because the measurements considered herein are from locations relatively close to the jet, there is a larger difference between these two sets of angles than for far-field measurements.

A ground-based array of 50 microphones, spaced $0.61\,m$ (2 ft) apart, was placed parallel to the engine's centerline at a sideline distance of $11.6\,m$ (approximately 38 ft). Their locations are marked as dots in Fig. [2]. GRAS Type I microphones, ranging from 3.18 to $6.35\,mm$ in diameter, were used in the reference array. This line array spanned approximately $30\,m$ in the z-direction and an angular aperture of $\theta = 53°–153°$.

Although jet operating conditions are not available for the various military engine powers, the nature of the

TABLE I. Relationship between angles, θ, cited herein, computed for an origin at the estimated dominant source region, z_0, and angles calculated for an origin at the nozzle exit, θ_e. All angles are measured relative to the jet engine inlet. For the sideline ground-based microphones located at angles θ, downstream distances from the nozzle exit, z, and downstream distance relative to z_0 are also listed.

θ	$z - z_0$ (m)	θ_e	z (m)
60°	−6.8 m	81°	−1.2
70°	−4.3 m	96°	1.2
80°	−1.8 m	108°	3.7
90°	0.0 m	115°	5.5
100°	1.8 m	122°	7.3
110°	4.3 m	130°	9.8
120°	6.7 m	136°	12.2
130°	9.7 m	142°	15.2
140°	14.0 m	149°	19.5
150°	18.3 m	156°	23.8

similarity spectra allows for a meaningful analysis. From Eqs. (1) and (2), the similarity spectra are calculated based on the peak frequency of the measured spectrum. While peak frequency is determined by the jet parameters, it is readily seen in the measured spectra, leaving only the amplitude to be determined, as in Eq. (4). This means that the jet velocity and temperature, although helpful in making explicit comparisons to laboratory studies, are not needed for this particular analysis.

IV. DATA ANALYSIS

The spectral content of the F-22 data has been analyzed at a variety of angles and distances for the four engine conditions: idle (Idle), intermediate (Int), military (Mil), and afterburner (AB). The data recorded on ground-based microphones indicate that the level, spectral shape, and peak frequency depend on both engine condition and direction. For all but Idle, there are many distances and angles at which large portions of the measured spectra are well approximated, at least in part, by the similarity spectra.

A. Spectral characteristics

The initial investigation into how well the similarity spectra match the F-22 data was performed with the ground-based microphones because they lack the interference nulls caused by ground reflections, which can complicate such comparisons. The angular variations in the spectra exhibit several important features of the radiated noise field. For example, Fig. 3 displays the spectra for AB on microphones placed at angles of $\theta = 60°$–150°, as measured relative to the engine inlet. Although the microphones at lesser angles are closer to the jet nozzle, the data recorded to the sideline of the jet have a lower peak level than data recorded farther downstream. This is not unexpected, due to the downstream directionality of the relatively intense Mach wave radiation. Additionally, the peak frequency decreases with increasing angle. Notice how the overall shape of the spectrum becomes more peaked (haystack-like) farther aft. This change in spectral shape with angle is representative of the difference between noise from fine-scale turbulent structures, detected close to the nozzle's sideline, and large-scale turbulent structures, which dominate the sound farther aft. However, at 150°, the portion of the spectrum near the peak frequency flattens out and the high-frequency portion seems elevated. While measurement environments, e.g., reflections, could be a cause, it is shown subsequently that this spectral shape, recorded at a ground-based microphone, can be explained by the two-source model.

One interesting feature of the AB data in Fig. 3 is that at many angles, there is evidence of a double peak in the spectrum. The presence of the double peak at these high levels is not accounted for by the similarity spectra for turbulent mixing noise. This could indicate a feature of a military-type jet engine not present in laboratory jet data or a feature unique to the near field. However, this same phenomena is also seen in far-field data from static measurements of the F/A-18E/F,[24,25] F-22A,[11] and F-35AA,[21] which suggests the former cause.

The angular dependence of the spectral shapes change with engine condition. Figure 4 displays the recorded sound pressure level (SPL) at four angles for Idle, Int, Mil, and AB on an absolute scale. The spectra at Idle and Int are truncated because higher frequencies contain tonal content that is not
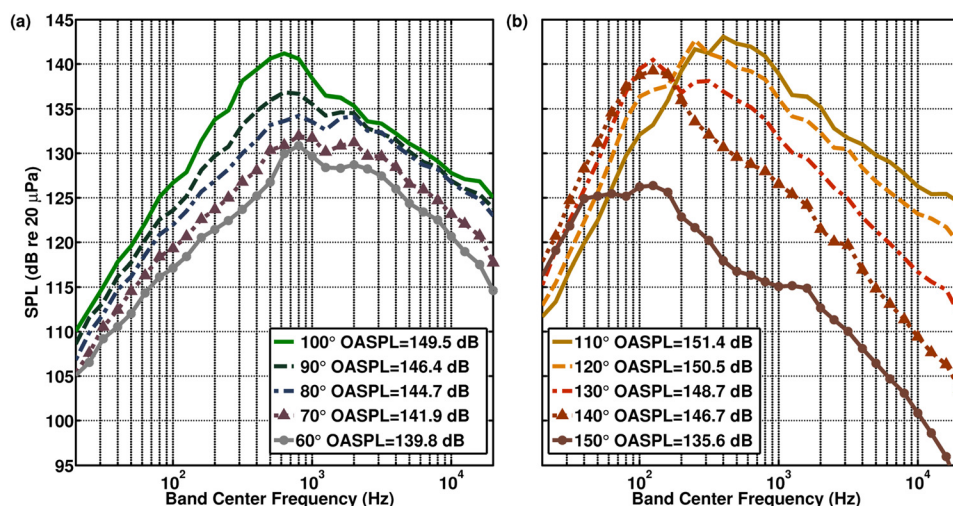

FIG. 3. (Color online) One-third octave band sound pressure levels measured at the ground-based microphones for the F-22 at afterburner. Angles, θ, are measured relative to the front of the aircraft and from the estimated region of dominant source strength shown as the "×" in Fig. 2.
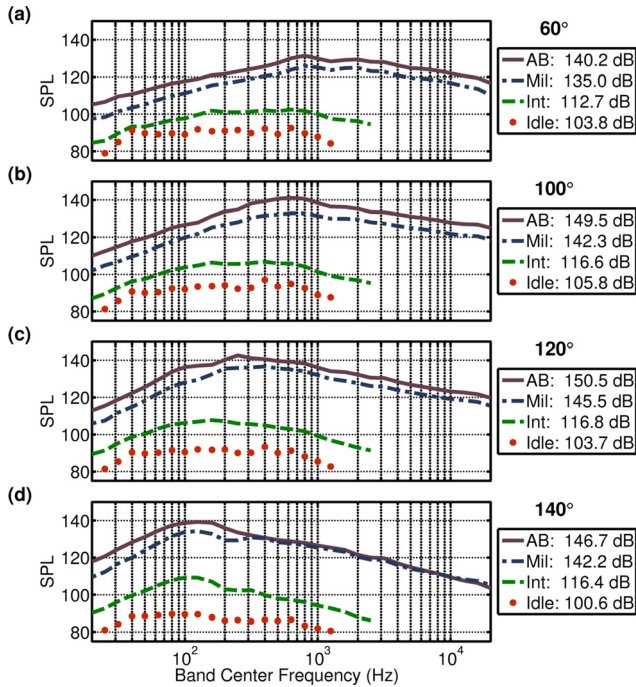
FIG. 4. (Color online) SPL (dB re 20 μPa) recorded on ground-based microphones at (a) 60°, (b) 100°, (c) 120°, and (d) 140° for four engine conditions: afterburner (solid), military (dash-dot), intermediate (dashed), and idle (dotted). The spectra at idle and intermediate power are truncated because higher frequencies contain tonal content that is not related to jet mixing noise.

related to jet mixing noise. At Idle, the spectral shape is fairly flat and similar at all angles, suggesting that the noise radiation is not dominated by jet mixing noise or that the two-jet interaction at Idle is significant because the second engine was also operating at Idle during the measurements. Thus, no further analyses are performed for Idle condition. The spectra for Int and Mil exhibit the same trends as AB: there is a noticeable difference between a more rounded spectral shape at sideline and a more peaked shape at larger angles. At lesser angles, there is a shift to a higher peak frequency as engine power increases, however, at 140° Int, Mil, and AB all have a peak frequency in/near the 125 Hz band. Viswanathan saw a similar constancy of peak frequency at far aft angles for dif-

ferent heated, subsonic jets in the laboratory.[26] Additionally, at 140°, the levels at Mil and AB above 300 Hz are almost identical. This reflects a difference in the maximum radiation direction, with that of Mil being farther aft.

B. Similarity spectra

The comparison between the spectra of jet noise measured on the ground-based microphones, located at a sideline distance of 11.6 m, and predictions from the similarity spectra are displayed in Figs. 5–7 for Int, Mil, and AB conditions, respectively. The spectra have been shifted by 25 dB for each ten-degree change in angle. The solid lines are the measured spectra; the dashed lines are the total predicted spectra. The estimated LSS and FSS contributions to the total predicted spectra are displayed as filled and open markers, respectively. It should be noted that the angles listed are relative to the estimated dominant source region 5.5 m from the nozzle exit. (See Fig. 2 and Table I for more details.)

At Int, shown in Fig. 5, the relative contributions of the FSS and LSS spectra to the total predicted spectrum follow the expected trends below the maximum analysis band of 2.5 kHz. At 60° and 70°, the measured spectrum is well represented by the FSS spectrum alone. From 80° to 120°, a gradual shift from an FSS-dominated spectrum to an LSS-dominated spectrum occurs. At 130°–140°, the LSS spectrum alone is needed to fit the data. At present, we have no explanation for the unusual spectral shape at 150°, which is LSS-like, but is more peaked in the maximum frequency region.

The comparisons between the measured and predicted spectra for military power in Fig. 6 and afterburner in Fig. 7 are similar. In both cases, the measured spectra at sideline can be largely represented by FSS(f, r). In cases where the measured spectra have a double peak, the best match for the low-frequency slope and the spread of the peak-frequency region, is found by selecting an $f_{r,G}$ in Eq. (4) between the two. However, at higher frequencies (above 4 kHz), the values of FSS(f, r) lie below the measured values. This difference grows with angle and engine power, as listed in Table II. Possible causes for this systematic high-frequency
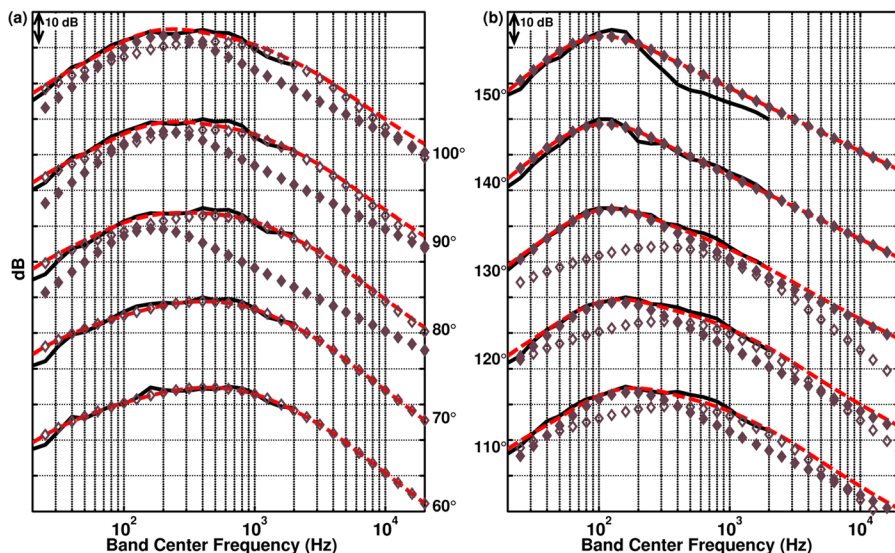

FIG. 5. (Color online) SPL recorded at ground-based microphones for intermediate power (80%) (solid lines), at the angles, θ, indicated, compared to the total predicted spectrum (dashed lines) and the contributions of the LSS (filled diamonds) and the FSS (open diamonds) similarity spectra.
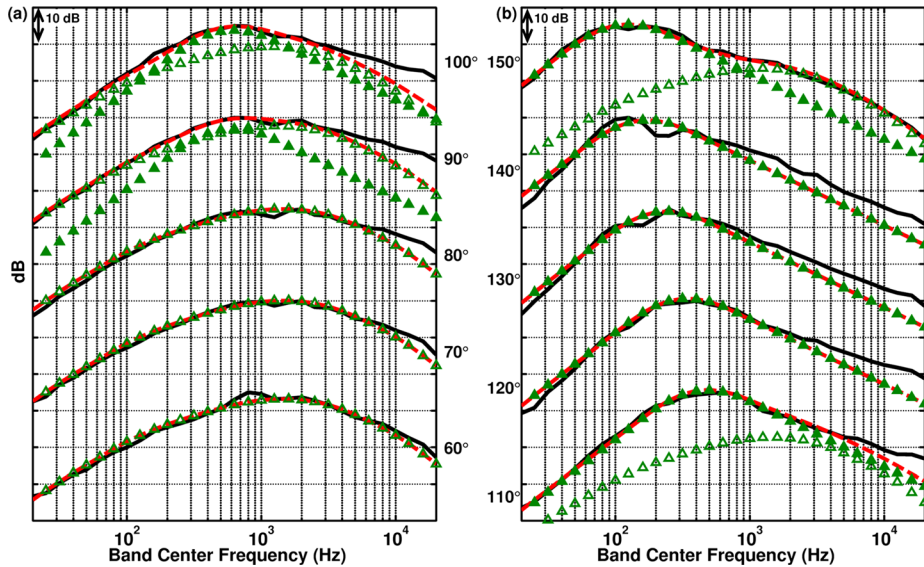
FIG. 6. (Color online) SPL recorded at ground-based microphones for military power (solid lines), at the angles, θ, indicated, compared to the total predicted spectrum (dashed lines) and the contributions of the LSS (filled triangles) and the FSS (open triangles) similarity spectra.

disagreement include atmospheric absorption, nozzle geometry and operating condition, and nonlinear propagation effects.

One might argue that a possible cause for the difference is that the similarity spectra were developed using data scaled to 100 D_j without explicitly including or excluding atmospheric attenuation, whereas these measurements were made close to the jet ($\sim$20 D_j to the sideline). However, the FSS and the 60° military spectra (in Fig. 7) agree within $\sim$2 dB at 20 kHz at this location. Given similar source regions for military and afterburner conditions, this agreement precludes attributing more than 2 of the 8 dB discrepancy at 20 kHz for the 60° afterburner case (Fig. 8) to this atmospheric absorption question. On the other hand, the systematic growth in the disagreement with increasing angle for afterburner towards the loudest region suggests an amplitude-related phenomenon may be responsible.

Although nozzle and jet operating conditions could be a contributing factor in the systematic shallow high-frequency slopes at Mil and AB, previous laboratory-scale studies with non-round nozzles and non-ideally expanded jets provided acceptable agreement with the similarity spectra.[13,18] In addition, as mentioned previously, Schlinker et al.[9] discussed other cases, which included ideally expanded supersonic jets from round nozzles, that had a shallower high-frequency slope than the LSS spectrum. Consequently, we believe the spectral slope differences may be attributed to nonlinear wave steepening causing an increase in energy at high frequencies, as has been seen in previous studies of the F-22A (Ref. 11) and F-35AA aircraft.[21,27] However, this behavior requires further investigation.

As predicted by Tam, at locations falling in the principal radiation region, the spectra are approximated solely by LSS($f, \mathbf{r}$), except for the double peaks and high-frequency discrepancies. Specifically, the agreement between the measured spectra at 110°–140° for AB and 120°–140° for Mil and LSS($f, \mathbf{r}$) is good at low frequencies and near the peak frequency. It is interesting to note that the 140° AB data matches the LSS($f, \mathbf{r}$) much better than 110°–130°. This improved match corresponds with the lower amplitudes beyond the maximum radiation region, as seen in Fig. 3.
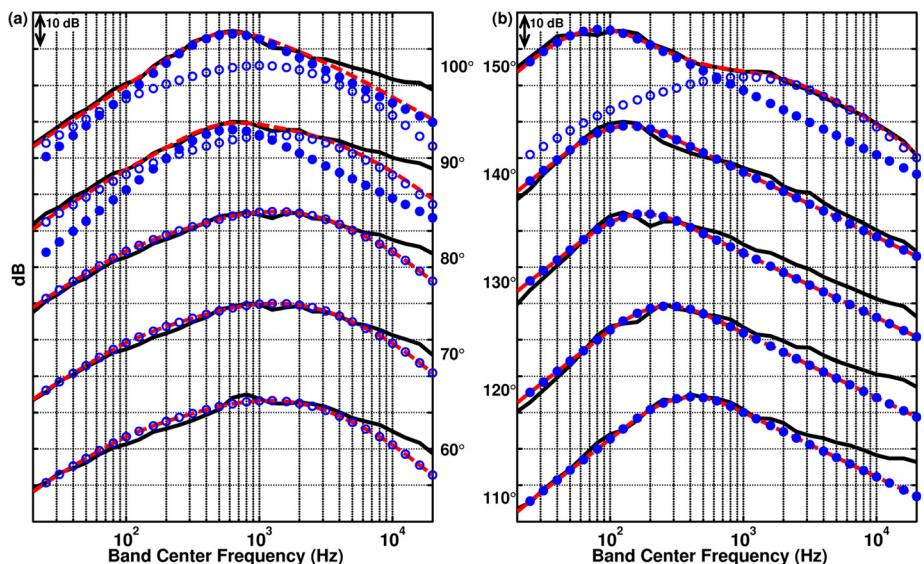

FIG. 7. (Color online) SPL recorded at ground-based microphones for afterburner (solid lines), at the angles, θ, indicated, compared to the total spectrum (dashed lines) and the contributions of the LSS (filled circles) and the FSS (open circles) similarity spectra.

TABLE II. Difference between the measured spectral levels and the total predicted spectral levels for the 20 kHz one-third octave band for military and afterburner conditions using ground-based microphones at a sideline distance of 11.6 m.

	Mil	AB
60°	2.1 dB	6.3 dB
70°	3.3 dB	5.2 dB
80°	6.2 dB	8.0 dB
90°	8.8 dB	8.6 dB
100°	8.7 dB	8.4 dB
110°	6.5 dB	9.7 dB
120°	7.2 dB	8.6 dB
130°	6.0 dB	5.9 dB
140°	6.0 dB	1.6 dB
150°	0.0 dB	0.5 dB

For Mil (Fig. 6) and AB (Fig. 7), the angular region where a combination of LSS(*f, r*) and FSS(*f, r*) is needed is narrower than for Int. Both types of mixing noise are needed to yield the best fit the spectra for Mil at 90°–110° and for AB at 90°–100°. While the presence of the double peaks in the spectra and shallower high-frequency slopes persist, the agreement below 4 kHz is remarkable. In addition to this transition region between the FSS-dominated noise region to the sideline and the LSS-dominated region in the principal radiation direction, the nature of the F-22 data for both Mil and AB changes again farther aft. Note that the increased temperature between the two conditions makes the Mach cone wider, and thus the transition from FSS to LSS occurs over a smaller range of angles.[26]

It can be seen in Fig. 6(b) (for Mil) and Fig. 7(b) (for AB) that the nature of the high- frequency noise changes dramatically from 140° to 150°. Instead of the relatively constant downward slope between 1 kHz and 20 kHz seen at 140°, the measured spectra at 150° exhibit a flatter region between 500 Hz and 1.5 kHz and a curved nature thereafter. This change in spectral shape can be accounted for by discerning that aft of the region of maximum radiation, the FSS

are again detectable. By using a combination of LSS(*f, r*) and FSS(*f, r*), the total predicted spectra track the interesting spectral shapes at 150°. This was unexpected as all previous comparisons in the literature show fits with the LSS spectrum at the largest measured angles: 160°.[3,12,16]

Figure 8 illustrates in more detail and with absolute levels the behavior at 150° and AB, where a combination of LSS(*f, r*) and FSS(*f, r*) is required to match the measured spectral shapes. Note that Fig. 7(b) showed a similar behavior for Mil power. Although the LSS accounts for nearly all of the overall sound pressure level (OASPL), the FSS contribution is essential to match the spectral shape above 400 Hz. It has not previously been observed that aft of the principal radiation region a combination of LSS and FSS noise is measureable. The reason the non-negligible contribution of the FSS noise is apparent in this experiment is that the far-field angles of maximum radiation of the F-22 are 125° at afterburner and 135° at military power.[11,28] These are farther forward than for other supersonic jets commonly reported in the literature. Thus, the design of the experiment and the shallower angles of maximum radiation region have provided, for the first time, a view of the type of sound field found closer to centerline, where both LSS(*f, r*) and FSS(*f, r*) are needed to predict the spectral shape of the noise at this location. However, it needs to be determined if the FSS contribution at far aft angles remains observable in the far field.

Another way to examine the relative contributions of the two types of turbulent mixing noise is by looking at the OASPL for each component. To our knowledge, this has only been carried out once previously,[4] even for laboratory-scale jets. Figure 9 shows the OASPL for the data (60°–150°) for all three engine conditions. Because the ground-based microphones were 11.6 m (38 ft) to the sideline of the jet, these OASPL values are near the foul line used by aircraft maintainers. The angular regions at which the OASPL curves have their maximum values (110°–120° for AB and 115°–125° for Mil) are different from the far-field observations of the maximum radiation direction (125° for AB and 135° for Mil).
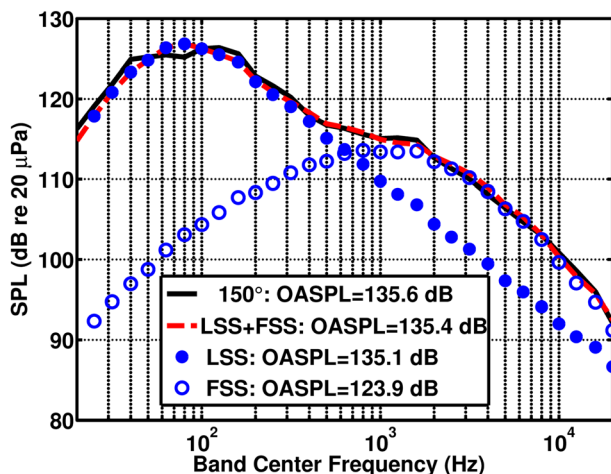

FIG. 8. (Color online) SPL for afterburner at 150° (solid line) compared to the LSS contribution (filled circles), the FSS contribution (open circles), and the total similarity spectrum prediction (dashed line)
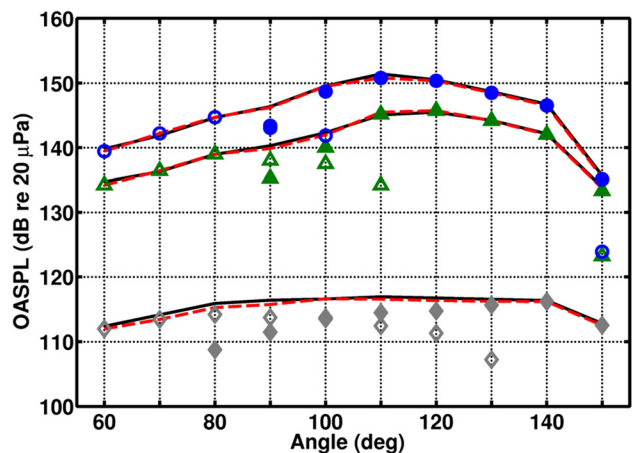

FIG. 9. (Color online) Overall sound pressure levels (OASPL) of data (solid lines), total predicted similarity spectrum (dashed lines), LSS contribution (filled), FSS contribution (open) for intermediate (diamonds), military (triangles), and afterburner power (circles). Note at that 100° for Int and 90° for AB, the filled and open markers have the same levels.

Also shown in Fig. 9 are OASPL for the total predicted spectra and the individual contributions of LSS(f, r) and FSS(f, r). The OASPL for the predicted spectra match the data extremely well because of the emphasis in matching the peak-frequency region. The OASPL for LSS(f, r) and FSS(f, r) indicate the relative strength of the two types of mixing noise and are equivalent to 10 log($\Sigma a(\mathbf{r})F(f_{r,F})$) and 10 log($\Sigma b(\mathbf{r})G(f_{r,G})$), where $a(\mathbf{r})$ and $b(\mathbf{r})$ are defined in Eq. (4). While the values chosen for $a(\mathbf{r})$ and $b(\mathbf{r})$ are determined empirically and, therefore, are not unique, they do yield predicted values for the total OASPL and spectral shapes that agree with the measured ones remarkably well (as shown in Figs. 5–7), except for the double peaks and shallower high-frequency slopes in the data.

The relative strengths of the OASPL for the LSS and FSS help to quantify the expected trends: (1) at sideline, the FSS contribute all the noise; (2) there is a region between the sideline and maximum radiation regions where the relative level of LSS noise increases while the FSS noise decreases; and (3) in the region of the Mach cone, the LSS account for all the noise. In addition, beyond the Mach cone, as the level of LSS decreases, the FSS, believed to be omnidirectional radiators distributed throughout the plume, are once again detectable at 150° for Mil and AB. Although the FSS OASPL is 10–12 dB lower than the LSS OASPL, the addition of the FSS makes a fundamental difference to the spectrum shape (see Fig. 8) because the two types of mixing noise have different peak frequencies.

The angular span over which a combination of two types of mixing noise is detectable changes with engine condition. For intermediate power, the OASPL for the LSS and FSS portions are within 10 dB from 80° to 120°. The contributions from the two types of noise are within about 10 dB at 90°–110° for Mil and 90°–100° for AB, and again for at 150° in both cases. This illustrates that the angles over which both types of noise are significant changes with engine power. Specifically, as the Mach number goes up, the transition region becomes narrower.

It is interesting to consider how the spatial variation of the OASPL curves displayed in Fig. 9 changes with engine condition. For Int, the OASPL is relatively flat across this angular aperture: there is only a difference of 4.6 dB between 60° [attributed to FSS(f, r)] and farther aft [attributed to LSS(f, r)]. For Mil and AB, however, there is a larger distinction between the levels associated with the two types of mixing noise. Specifically, the OASPL varies by 11.6 dB for Mil and by 15.9 dB for AB. It is interesting to note that there is less variation with angle in the FSS OASPL (4.8 dB for Mil and 5.3 dB for AB) than for the LSS OASPL (12.4 for Mil and 15.7 for AB). This was also noted in the comments regarding Fig. 6 of Ref. 4: there is a larger variation in the LSS contributions to the OASPL for heated, supersonic jets. A possible physical reason for this is likely that the stronger Mach wave radiation in heated, supersonic jets[4] boosts the efficiency of the sound generation associated with the LSS, which in turn causes an increase in the corresponding OASPL.

Another interesting feature shown in Fig. 9 concerns an indirect estimation regarding the dominant source region for the FSS noise. In the experimental set-up, the angles were measured relative to the engine inlet and a position 5.5 m downstream from the nozzle exit (shown as the "×" in Fig. 2). This was chosen to be consistent with observations from previous measurements,[9,11] while recognizing that the "origin" for the distributed source region depends on frequency and engine condition. In line with the assumption that the FSS are comprised of omnidirectional radiators, the fact that the FSS-based OASPLs have greatest values at 80° for all three engine conditions may indicate that the dominant source region for the FSS is upstream of the chosen origin. This agrees with the results in Ref. 9 where beamforming indicated that the dominant source region for higher frequencies was closer to the nozzle than for lower frequencies. However, as FSS is only a minor contributor to the overall sound levels radiated by the jet, it is understandable that previous analyses for detecting a single dominant source region for the jet place it closer to the chosen origin.

V. CONCLUDING DISCUSSION

The empirical similarity spectra[3] for the two sources of turbulent mixing noise, the large (LSS) and fine-scale (FSS) turbulent structures, exhibit a large degree of congruity with the noise from an F-22A Raptor recorded at a near-field sideline array of ground-based microphones for three engine conditions: intermediate (80%), military, and afterburner. The comparison over a broad range of angles is remarkable considering the non-ideally expanded nature of the jet and complicated engine geometry, and the fact that the similarity spectra were initially developed using only far-field data from ideally expanded, laboratory jets. The analysis provides both physical insight and directions for further research.

The favorable agreement demonstrates the relative importance of turbulent mixing noise in full-scale engines. Specifically, this analysis of F-22 noise near the jet over a wide angular aperture shows that mixing noise dominates the spectrum, despite the non-ideally expanded conditions. The one-third octave band spectra lack concrete evidence of broadband shock associated noise, as is typically observed to the sideline of laboratory- scale jets operated at nonideally expanded, supersonic conditions.[2,29] An additional feature that requires investigation is the double-peaked nature of the aft spectra, which has not been observed in laboratory-scale jets.

The study has also provided clear evidence that the FSS spectrum is not only important to the sideline of the jet, upstream of the Mach cone where the LSS is dominant, but also downstream as well. The 150° data for both military and afterburner exhibit high-frequency spectral behavior that can be modeled extremely well across the bandwidth of interest when the FSS and LSS spectra are combined. The reason these data lend themselves to the observation that beyond the region of loudest sound radiation the omnidirectional FSS contribution can be detected, is that the F-22 engine has far-field maximum radiation directions of 125° for afterburner and 135° for military power,[11] which are farther from the centerline than most other full-scale engines and laboratory jets. While this observation serves as additional support for the omnidirectional radiation of the fine-scale structures,[3] it seemingly contradicts the current

interpretations of the characteristics of the fine-scale radiation as described in the literature.[2,8,15,30] Mean-flow effects have been believed to produce a fine-scale, cone of silence in the aft direction, beyond which only the LSS radiation is important. Observations of the FSS spectral shape in the far aft direction shown here may cause that theory to be revisited. Additional investigations may involve examination of the far-field spectra at large angles for similar behavior.

This work was introduced by observing that previous far-field studies (e.g., see Ref. 9) had shown shallower high-frequency slopes in the maximum radiation direction than predicted by the LSS similarity spectra. While there is a substantial need for further investigation, it has been established that at military and afterburner conditions, the high-frequency slopes of the measured spectra in the geometric near field are not only shallower than the LSS in the principal radiation region, but also shallower than the FSS at lesser angles. Further study is required to determine the relative importance of atmospheric absorption and nonlinear effects as a function of angle and range. This will help connect previous far-field observations to the near-field noise environment and better establish whether the discrepancy is a propagation or source phenomenon, or perhaps both.

ACKNOWLEDGMENTS

[1]C. K. W. Tam, "Supersonic jet noise," Annu. Rev. Fluid Mech. **27**, 27–43 (1995).

[2]C. K. W. Tam, "Jet noise: Since 1952," Theor. Comput. Fluid Dyn. **10**, 393–405 (1998).

[3]C. K. W. Tam, M. Golebiowsky, and J. M. Seiner, "On the two components of turbulent mixing noise from supersonic jets," AIAA Paper No. 96-1716 (1996).

[4]C. K. W. Tam, K. Viswanathan, K. K. Ahuja, and J. Panda, "The sources of jet noise: experimental evidence," J. Fluid Mech. **615**, 253–292 (2008).

[5]K. Viswanathan and M. J. Czech, "Role of jet temperature in correlating jet noise," AIAA J. **47**, 1090–1106 (2009).

[6]R. H. Schlinker, *Supersonic Jet Noise Experiments*, Ph.D. dissertation, University of Southern California, 1975.

[7]J. Laufer, R. Schlinker, and R. E. Kaplan, "Experiments on supersonic jet noise," AIAA J. **14**, 489–498 (1976).

[8]C. K. W. Tam, N. N. Pastouchenko, and R. H. Schlinker, "Noise source distribution in supersonic jets," J. Sound Vib. **291**, 192–201 (2006).

[9]R. H. Schlinker, S. A. Liljenberg, D. R. Polak, K. A. Post, C. T. Chipman, and A. M. Stern, "Supersonic jet noise source characteristics & propagation: Engine and model scale," AIAA Paper No. 2007-3623 (2007).

[10]B. P. Petitjean and D. K. McLaughlin, "Experiments on the nonlinear propagation of noise from supersonic jets," AIAA Paper No. 2003-3127 (2003).

[11]K. L. Gee, V. W. Sparrow, M. M. James, J. M. Downing, C. M. Hobbs, T. B. Gabrielson, and A. A. Atchley, "The role of nonlinear effects in the propagation of noise from high-power jet aircraft," J. Acoust. Soc. Am. **123**, 4082–4093 (2008).

[12]K. Viswanathan, "Analysis of the two similarity components of turbulent mixing noise," AIAA J. **40**, 1735–1744 (2002).

[13]C. K. W. Tam and K. Zaman, "Subsonic noise from nonaxisymmetric and tabbed nozzles," AIAA J. **38**, 592–599 (2000).

[14]K. Viswanathan, "Investigation of noise source mechanisms in subsonic jets," AIAA J. **46**, 336–355 (2008).

[15]R. H. Schlinker, J. C. Simonich, D. W. Shannon, R. A. Reba, T. Colonius, K. Gudmundsson, and F. Ladeinde, "Supersonic jet noise from round and chevron nozzles: Experimental studies," AIAA Paper No. 2009-3257 (2009).

[16]M. D. Dahl and D. Papamoschou, "Analytical predictions and measurements of the noise radiated from supersonic coaxial jets," AIAA J. **38**, 584–591 (2000).

[17]J. Morgan, T. B. Neilsen, K. L. Gee, A. T. Wall, and M. M. James, "Simple-source model of high-power jet aircraft noise," Noise Control Eng. J. **60**, 435–449 (2012).

[18]C. K. W. Tam, "Influence of nozzle geometry on the noise of high-speed jets," AIAA J. **36**, 1396–1400 (1998).

[19]A. T. Wall, K. L. Gee, M. M. James, K. A. Bradley, S. A. McInerny, and T. B. Neilsen, "Near-field noise measurements of a high-power jet aircraft," Noise Control Eng. J. **60**, 421–434 (2012).

[20]M. M. James and K. L. Gee, "Aircraft jet plume source noise mesurement system," Sound Vib. **44**, 14–17 (2010).

[21]K. L. Gee, J. M. Downing, M. M. James, R. C. McKinley, R. L. McKinley, T. B. Neilsen, and A. T. Wall, "Nonlinear evolution of noise from a military jet aircraft during ground run-up," AIAA Paper No. 2012-2258 (2012).

[22]J. C. Yu and D. S. Dosanjh, "Noise field of a supersonic mach 1.5 cold model jet," J. Acoust. Soc. Am. **51**, 1400–1410 (1972).

[23]A. T. Wall, K. L. Gee, T. B. Neilsen, D. W. Krueger, M. M. James, S. D. Sommerfeldt, and J. D. Blotter, "Full-scale jet noise characterization using scan- based acoustical holography," AIAA Paper 2012-2081, June 2012.

[24]K. L. Gee, T. B. Gabrielson, A. A. Atchley, and V. W. Sparrow, "Preliminary analysis of nonlinearity in military jet aircraft noise propagation," AIAA J. **43**, 1398–1401 (2005).

[25]B. Greska and A. Krothapalli, "On the far-field propagation of high-speed jet noise," in *ASME 2008 Noise Control and Acoustics Division Conference* (2008).

[26]K. Viswanathan, "Aeroacoustics of hot jets," J. Fluid Mech. **516**, 39–82 (2004).

[27]K. L. Gee, T. B. Neilsen, J. M. Downing, M. M. James, R. L. McKinley, R. C. McKinley, and A. T. Wall, "Near-field shock formation in noise propagation from a high-power jet aircraft," J. Acoust. Soc. Am. **133**, EL88–EL93 (2013).

[28]Air Force Research Laboratory, NOISEFILE Database, Wright-Patterson AFB, OH (2003).

[29]K. A. Viswanathan, M. B. Alkislar, and M. J. Czech, "Characteristic shock component of jet noise," AIAA J. **48**, 25–46 (2010).

[30]R. H. Schlinker, R. A. Reba, J. C. Simonich, T. Colonius, K. Gudmundsson, and F. Ladeinde, "Towards prediction and control of large scale turbulent structure supersonic jet noise," in *2009 ASME Turbo Expo*, American Society of Mechanical Engineers, Orlando, FL (2009), pp. 217–229.